Ground-Based Experiments on Vibrational Thermal Convection

Michael F. Schatz, Jeffrey L. Rogers, School of Physics, Georgia Institute of Technology, Atlanta, GA 30332-0430, USA, mike.schatz@physics.gatech.edu

1. INTRODUCTION

In many microgravity experiments involving fluid flow, density variations arise frequently due to, for example, temperature or concentration gradients. These variations couple to time-dependent accelerations (g-jitter) that are unavoidably present aboard spacecraft; this coupling can significantly influence outcomes in microgravity experiments. Ground-based experiments can provide insight into these effects that complements both theoretical studies and space-based experiments.

Convective flow is one class of behavior that can arise from g-jitter effects. The Rayleigh-Benard system is an important model for understanding thermal convection; thus, studies of this problem in the presence of acceleration modulations provide insight into the nature of g-jitter induced flow and of the effects of modulation and noise on non-equilibrium pattern formation.

In the following, we describe experiments on Rayleigh-Benard convection subjected to sinusoidal acceleration modulation. Theoretical investigations of this problem have been conducted by several workers [1-3]; by comparison there appears to be little previous experimental work [3].

2. DESCRIPTION OF EXPERIMENT

CO_2 gas, compressed at 3.10 E10^6 PA, is confined to a horizontal layer of depth $d = 0.064$ cm by a 0.5 cm thick aluminum mirror and a 2.54 cm thick sapphire window (Fig. 1). The thickness of the gas layer varies by approximately 1 μm, as measured inteferometrically. A cylindrical paper sidewall of inner diameter $2, d = 4.13$ cm bounds the gas layer laterally.

The convective flow is controlled by applying a temperature difference ΔT across the layer and by oscillating the layer vertically with a sinusoidal acceleration of frequency f and amplitude a. ΔT, which typically ranges from 20 to 30 °C, is applied uniformly by heating the mirror and cooling the window. The temperature of the bottom plate fluctuates by less than 0.003 °C, while the window, whose temperature is fixed at 22.4 °C, is regulated to 0.01 °C. The dimensionless number that characterizes the heating is the Rayleigh number $R = \frac{g\alpha\Delta T d}{\nu\kappa}$ with kinematic viscosity ν, thermal diffusivity κ, temperature coefficient of volumetric expansion α and the earth's gravitational acceleration g. We describe our results in terms of a reduced Rayleigh
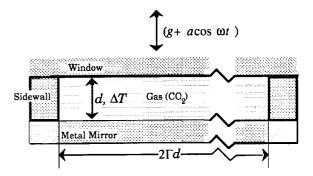

Figure 1: Geometry of Rayleigh-Bénard convection subjected to time periodic acceleration modulations.

number $\epsilon = \frac{R - R_0}{R_0}$ where $R_0 = 1708$ is the Rayleigh number at the onset of convection in the absence of shaking. Time dependent accelerations are applied by a hydraulic shaker table that vertically vibrates the experiment. In typical experiments, a ranges from 1 to 8 g and 8 Hz $<= f <= 21$ Hz; f is controlled to within 0.01 Hz and a is maintained to within 5%. The vertical diffusion time $\frac{d^2}{\kappa}$ (≈ 1 s) is used to obtain the nondimensional frequency $\omega = \frac{2\pi f d^2}{\kappa}$; the oscillation amplitude is conveniently described in terms of the nondimensional displacement $\delta = \frac{a}{g\omega^2}$. The Prandtl number is fixed at 0.9 in the experiments.

The convection flow is visualized by the shadowgraph technique. Dynamics that occur over long time scales ($>> \frac{2\pi}{\omega}$) are captured using a standard NTSC video camera interfaced to a frame grabber. The camera is shuttered by a ferroelectric liquid crystal polarizer that is synchronized with the drive signal for the shaker table. Fast ($< \frac{2\pi}{\omega}$) convective dynamics can be captured using a high speed (800 frames per second) video camera. In all cases, the shadowgraph images are digitized and enhanced to improve the signal-to-noise using standard image processing techniques.

3. RESULTS

A wide variety of convective flow states are observed for fixed ω (Fig. 2). Each experimental run is performed by setting ϵ to a fixed value and slowly ramping up and then down in δ. A range of ϵ is probed by repeating this procedure at different values of ϵ. Each experimental run begins with $\delta = 0$ where the convective flow is in
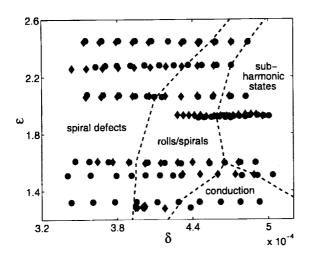
Figure 2: Phase diagram of convective flows is obtained by plotting the reduced Rayleigh number ϵ as a function of displacement amplitude δ with drive frequency $\omega =$ 80. Data is obtained by fixing ϵ and varying δ; increasing δ is indicated by closed circles and decreasing δ is indicated by closed diamonds. The boundaries between flow states (dotted lines) are approximate and are drawn in to guide the eye.

the disordered, time dependent spiral defect chaos [4] for the range of ϵ described here.

As δ increases for low values of ϵ, the system passes through a sequence of increasingly ordered convective flows and returns to the conduction state (Figs. 2 and 3). Initially, the number of spiral defects decrease and the convection pattern exhibits either a single spiral (Fig. 3(b)) or a pattern of straight rolls (Fig. 3(c)). Upon further increases of δ, hexagonal patterns are observed to arise for a narrow range of δ (Fig. 3(d), but not shown on the phase diagram Fig. 2); hexagons disappear and the conduction state returns for δ sufficiently large. In this regime, all convective patterns are similar in appearance to those flows that arise in standard Rayleigh-Benard convection (the "no-shake" case) with the exception that in the presence of shaking, all convective patterns in this range of parameter are observed to oscillate synchronously with the drive frequency ω. (Patterns near onset in standard Rayleigh-Benard convection are stationary.).

The conduction state becomes unstable to new convective patterns with further increases in δ for low values of epsilon (Fig. 4). These new convective patterns are observed to oscillate at $\omega/2$, the subharmonic of the drive frequency. The subharmonic flows initially appear as
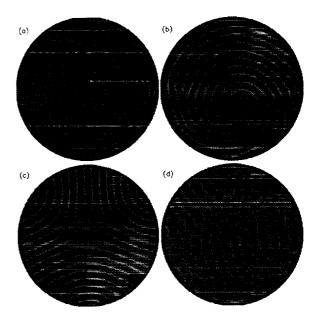

Figure 3: Transitions between convective flows with time dependence synchronous with the drive frequency ω. The convective flow exhibits spiral defect chaos in the absence of modulation, as shown in (a) for $\epsilon =$ 1.13. The convective flow becomes less disordered as the displacement amplitude δ of the modulation is increased, giving rise to patterns in the form of (b) spirals ($\delta = 4.56E10^{-4}$, $\omega = 79$, $\epsilon = 2.06$), (c) stripes ($\delta = 1.58E10^{-4}$, $\omega = 181$, $\epsilon = 2.26$), or (d) hexagons ($\delta = 1.70E10^{-4}$, $\omega = 178$, $\epsilon = 2.44$). All cases of modulated convection (b-d) exhibit global rotation of the pattern. For these values of ϵ and ω, the system returns to the conduction state with further increases in δ.
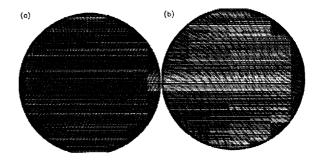

Figure 4: Convective flows with temporal response at the subharmonic $\frac{\omega}{2}$. The subharmonic patterns appear as (a) stripes ($\delta = 4.82E10^{-4}$, $\omega = 80$, $\epsilon = 1.92$), with wavelengths substantially smaller than that of unmodulated or synchronous convection (Fig. 1). Upon further increases in δ, the stripes become wavy (c). In both cases, the patterns exhibit global rotation.

nearly straight rolls with a wavelength that is significantly smaller than the synchronous roll patterns(Fig. 4(a)). With further increases in δ the subharmonic rolls become wavy along the roll direction; this waviness is accompanied by an additional frequency.

A global rotation to the pattern is observed for both synchronous and subharmonic ordered patterns. The direction of rotation depends on initial conditions; both clockwise and counterclockwise pattern rotations have been observed for all patterns. The rotation rate is observed to slow as δ approaches values near the transition to conduction.

Some aspects of these transitions can be understood drawing an analogy with the motion of a damped simple pendulum whose pivot is subjected to vertical sinusoidal oscillation [1]. In the absence of shaking, an inverted pendulum that is unstably balanced above the pivot is akin to a fluid layer where the conduction state is destabilized by heating from below. It is known that an inverted pendulum may be stabilized if the pivot is subjected to oscillations; the circumstances under which this may arise can be determined examining the stability of the equation of motion, the Mathieu equation. In the same way, it may be expected that oscillations may stabilize the conduction state in the Rayleigh-Benard problem. This analogy can be made quantitative; an approximate linear stability of the fluid layer can be performed by mapping equations of motion for the fluid layer to the Mathieu equation [1]. Both subharmonic and fundamental modes that are observed in the experiment are predicted with approximate values for the onset of convection and the wavenumbers that are consistent with the experiments.

For sufficiently large values of ϵ, there is no range of δ where the conduction state exists and the fundamental mode increases for low values of epsilon, the system can pass directly from the fundamental mode to the subharmonic mode of convection (Fig. 5.). As δ is increased, the sequence of fundamental modes are similar to those observed at smaller ϵ. For δ sufficiently large, the subharmonic modes first appear in localized regions--typically trapped within defects of the fundamental pattern. These subharmonic can be trapped because they have a significantly smaller length scale than the fundamental mode; moreover, the subharmonics are advected with the defects in the fundamental mode and appear and disappear as the defects in the fundamental pattern appear and disappear (Fig. 5 (a)). With further increases in δ, the subharmonic pattern spreads throughout the convection cell; both patterns are seen to coexist (Fig. 5(b)). The patterns coexist
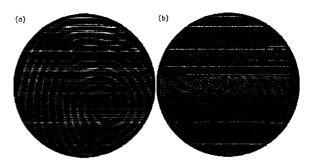

Figure 5: Competition between synchronous and subharmonic patterns. The subharmonic stripes first appear as localized patches trapped within defects of the synchronous pattern (a) ($\delta = 4.71E10^{-4}$, $\omega = 80$, $\epsilon = 2.27$). With small changes in parameter, both subharmonic and synchronous patterns coexist over most of the apparatus (b).

for only a small range of δ with further increases in δ, subharmonic patterns of straight rolls appear.

4. CONCLUSIONS

Our experiments on Rayleigh-Benard convection with periodic acceleration modulation are permitting the study of flows that arise from two different pattern forming mechanisms. We observe flows that respond synchronously with the drive frequency ω; the patterns observed in this regime have wavenumbers and morphologies that are similar to convection in the absence of modulation, where the wavenumber selection is known to be directly related to the geometry. We also observe flows that respond at the drive frequency's subharmonic $\frac{\omega}{2}$ and have wavenumbers that are substantially smaller than those for the fundamental modes; the temporal behavior of the subharmonic patterns is akin to those observed in systems subject to parametric instability (e.g. surface waves in Faraday experiments) where wavenumbers are selected through a dispersion relation. Our experimental results for the onset of convection appear to be in agreement with preliminary computations of the approximate linear stability [1] of the conduction state; we are currently refining the computations for the exact problem [2].

To make closer connection to the effects of g-jitter in a microgravity environment, we will extend our studies to include stochastic modulations (noise). It is well-known that acceleration fluctuations aboard spacecraft exhibit both deterministic and stochastic features [5]. Our experiments on Rayleigh-Benard convection with acceleration modulation provide a general setting to

understand the effects of noise on convective flows. Specifically, recent theoretical work suggests that small amounts of noise can alter qualitatively transitions to oscillatory states [6]. We will investigate this question in future experiments.

5. ACKNOWLEDGMENTS

6. REFERENCES

1. P. M. Gresho and R. L. Sani, J. Fluid Mech., **40**, 783 (1970).

2. R. M Clever, G. Schubert and F. H. Busse, J. Fluid Mech., **253**, 663 (1993).

3. G. Z. Gershuni and D. V. Lyubimov, *Thermal Vibrational Convection* (J. Wiley, Chichester, England, 1998).

4 J. R. de Bruyn, E. Bodenschatz, S. W. Morris, S. P. Trainoff, Y. Hu, D. S. Cannell and G. Ahlers, Rev. Sci. Instrum., **67**, 2043 (1996) and references therein.

5. J. R. Thomson, J. Casademunt, F. Drolet, and J. Vinals, Phys. Fluids, **9**, 1336 (1997).

6. F. Drolet, and J. Vinals, Phys. Rev. E, **56**, 2649 (1997).